CGC/saturation approach: Secondary Reggeons and $\rho = \mathrm{Re}/\mathrm{Im}$ dependence on energy

E. Gotsman [a,*], E. Levin [a,b], I. Potashnikova [b]

[a] *Department of Particle Physics, School of Physics and Astronomy, Raymond and Beverly Sackler Faculty of Exact Science, Tel Aviv University, Tel Aviv, 69978, Israel*
[b] *Departemento de Física, Universidad Técnica Federico Santa María, and Centro Científico-Tecnológico de Valparaíso, Avda. Espana 1680, Casilla 110-V, Valparaíso, Chile*

A R T I C L E   I N F O

A B S T R A C T

In this letter we demonstrate that a model based on the CGC/saturation approach, successfully describes soft interaction collisions for the wide range of $W = \sqrt{s} = 30$ GeV ÷ 13 TeV including the new TOTEM data at 13 TeV. We have now incorporated the secondary Reggeons in our approach this enables us to describe the complete set of the soft data, including the energy behavior of ρ the ratio of the real to imaginary parts of the elastic scattering amplitude. We argue that it is premature to claim that an odderon contribution is necessary, but estimate its possible strength as 1 mb to the real part of the amplitude at $W = 13$ TeV. We show that the odderon contribution depends on the value of energy leading to Re $A(s, t = 0) = 8$ mb at $W = 21.2$ GeV. Bearing this in mind we do not believe that ρ at high energies is the appropriate observable for detecting the odderon contribution. The successful description of the soft data in the wide range of energy strengthens our claim that the CGC/saturation approach is the only viable candidate for an effective theory for high energy QCD.

1. Introduction

In our recent papers [1,2] we have constructed a model, which allows us to discuss soft and hard processes on the same footing. This model is based on the CGC/saturation approach (see Ref. [3] for a review) and on our previous attempts to build such a model [4–11].

The model, that we proposed in Refs. [1,2], successfully describes the DIS data from HERA, the total, inelastic, elastic and diffractive cross sections, the t-dependence of these cross sections, as well as the inclusive production and rapidity and angular correlations in a wide range of high energies up to 13 TeV. In this letter we include in our formalism the contribution of the secondary Reggeons that allows us to expand the region of energies down to $W = 50$ GeV. The main motivation for this is our need to describe the energy behavior of the ratio $\rho = \mathrm{Re}/\mathrm{Im}$ of the scattering amplitude, to which the secondary reggeons make a significant contribution. The new TOTEM data [12] shows that the value of

$\rho = 0.1 \pm 0.01 (0.09 \pm 0.01)$ is lower than expected, and this ignited the hot discussion about the possible contribution of the odderon [13–20]. The odderon contribution to the negative signature appears naturally in perturbative QCD, with an intercept which is equal to zero [21,22]. In other words, we expect that the odderon will lead to a constant real part of the scattering amplitude at high energy, while the other contributions from the pomeron and the secondary reggeons result in a decreasing real part. Consequently, it is apt to elucidate the odderon contribution by investigating ρ at high energies.

The main result of this letter is (i) that $\rho \approx 0.1$ at $W = 13$ TeV appears naturally in our approach without having to assume an odderon contribution; and (ii) the value of its possible contribution is about 1 mb in the real part of the scattering amplitude, independent of energy. The small and decreasing value of ρ at high energies stems from the CGC motivated amount of shadowing (screening) corrections and furnishes strong support for our approach.

Our model incorporates two ingredients: the achievements of the CGC/saturation approach, and the pure phenomenological treatment of the long distance non-perturbative physics, necessary, due to the lack of theoretical understanding of the confinement of quark and gluons.
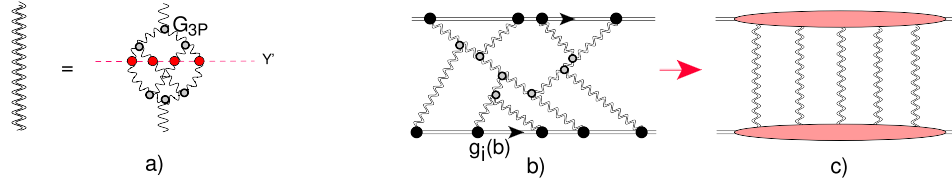
Fig. 1. Fig. 1(a) shows the set of diagrams in the BFKL Pomeron calculus that produce the resulting (dressed) Green function of the Pomeron in the framework of high energy QCD. The red blobs denote the amplitude for the dipole–dipole interaction at low energy. In Fig. 1(b) the net diagrams, which include the interaction of the BFKL Pomerons with colliding hadrons, are shown. The sum of the diagrams after integration over positions of G_{3P} in rapidity, reduces to Fig. 1(c). The wavy lines denote the BFKL Pomerons, while the double wavy lines describe the dressed Pomerons.

2. The model: theoretical background for BFKL Pomerons and their interaction

In Ref. [23] it is shown that at high energy, but in the energy range:

$$Y \leq \frac{2}{\Delta_{\text{BFKL}}} \ln\left(\frac{1}{\Delta_{\text{BFKL}}^2}\right). \tag{1}$$

Pomerons and their interactions, determine the scattering amplitude. In other words, it is shown that in this energy range the CGC approach and the BFKL Pomeron calculus are equivalent. In this paper it is also been shown that we can use the MPSI approximation [24], to find the dressed Green function of the BFKL Pomeron ($G^{\text{dressed}}(r, Y - Y_0, \boldsymbol{b})$). This Green function exhibits a geometric scaling behavior, being function of one variable $\tau = r^2 Q_S^2(Y, b)$, where r denotes the size of the colorless dipole and Q_s the saturation momentum; and it can be found using the solution to the non-linear Balitsky–Kovchegov equation [25].

Based on the above results we constructed a model [1,2,4,5, 26] which describes the soft interaction at high energy in the region given by Eq. (1). In this equation Δ_{BFKL} denotes the intercept of the BFKL Pomeron. It turns out that in our model $\Delta_{\text{BFKL}} \approx 0.2 - 0.25$ leading to $Y_{max} = 20 - 30$, which covers all collider energies. The procedure of calculation of $G^{\text{dressed}}(r, Y - Y_0, \boldsymbol{b})$ is shown in Fig. 1(a), which illustrates the MPSI approximation. The 'fan' Pomeron diagrams in Fig. 1(a) correspond to the solution of the nonlinear BK equation. We found a numerical solution to the BK equation, and an analytical formula that describes this solution to within 5% accuracy (see Refs. [1,2,4,26]). Finally,

$$G^{\text{dressed}}(G_P(z)) = a^2(1 - \exp(-G_P(z))) + 2a(1-a)\frac{G_P(z)}{1 + G_P(z)}$$
$$+ (1-a)^2 \widetilde{G}(G_P(z)) \tag{2}$$

with $\widetilde{G}(T) = 1 - \frac{1}{T}\exp\left(\frac{1}{T}\right)\Gamma\left(0, \frac{1}{T}\right)$ where $\Gamma(s, z)$ is the upper incomplete gamma function (see Ref. [27] formula 8.35). $G_P(z)$ denotes the BFKL Pomeron in the vicinity of the saturation scale:

$$G_P(z) = \phi_0 \left(r^2 Q_s^2(Y - Y_0, b)\right)^{1-\gamma_{cr}}. \tag{3}$$

$a = 0.65$ for the solution of the BK equation. For the saturation momentum we use the following general formula

$$Q_s^2(b, Y) = Q_{0s}^2(b, Y_0) e^{\lambda(Y - Y_0)} \text{ where } Q_{0s}^2(b, Y_0) = \left(m^2\right)^{1-1/\bar{\gamma}}$$
$$\times (S(b, m))^{1/\bar{\gamma}} \text{ with } S(b, m) = \frac{m^2}{2\pi} e^{-mb}. \tag{4}$$

In Eq. (2)–Eq. (4) we know from leading order perturbative QCD, that $\lambda = 4.8\bar{\alpha}_S$ and $\bar{\gamma} = 1 - \gamma_{cr} = 0.63$. ϕ_0 and m are the phenomenological parameters which determine the value of the Pomeron Green function at $\tau = 1$ (from Fig. 1(a) one can see that $\phi_0 \propto$ dipole–dipole amplitude) and the typical dimensional scale

at $Y = Y_0$. In Eq. (4) we specify the large impact parameter behavior which cannot be derived from CGC approach [28]. The form of b dependence is purely phenomenological, while the exponential decrease at large b follows from the Froissart theorem [29].

3. The model: phenomenological input for the hadron structures

However, we cannot build the scattering amplitude without a phenomenological input for the structure of the scattering hadrons. For this, we use a two channel model, which allows us to calculate the diffractive production in the region of small masses. In our model, we replace the rich structure of the diffractively produced states, by a single state with the wave function ψ_D, a la Good–Walker [30]. The observed physical hadronic and diffractive states are written in the form

$$\psi_h = \alpha \Psi_1 + \beta \Psi_2; \qquad \psi_D = -\beta \Psi_1 + \alpha \Psi_2;$$
$$\text{where} \quad \alpha^2 + \beta^2 = 1. \tag{5}$$

Functions Ψ_1 and Ψ_2 form a complete set of orthogonal functions $\{\Psi_i\}$ which diagonalize the interaction matrix T

$$A_{i,k}^{i'k'} = < \Psi_i \Psi_k |\mathbf{T}|\Psi_{i'} \Psi_{k'} > = A_{i,k} \delta_{i,i'} \delta_{k,k'}. \tag{6}$$

The unitarity constraints have the form

$$2 \, \text{Im} \, A_{i,k}(s, b) = |A_{i,k}(s, b)|^2 + G_{i,k}^{in}(s, b), \tag{7}$$

where $G_{i,k}^{in}$ denotes the contribution of all non diffractive inelastic processes, i.e. it is the summed probability for these final states to be produced in the scattering of a state i off a state k. In Eq. (7) $\sqrt{s} = W$ denotes the energy of the colliding hadrons, and b the impact parameter. A solution to Eq. (7) at high energies, has the eikonal form with an arbitrary opacity Ω_{ik}, where the real part of the amplitude is much smaller than the imaginary part.

$$A_{i,k}(s, b) = i \left(1 - \exp\left(-\Omega_{i,k}(s, b)\right)\right),$$
$$G_{i,k}^{in}(s, b) = 1 - \exp\left(-2\,\Omega_{i,k}(s, b)\right). \tag{8}$$

Eq. (8) implies that $P_{i,k}^S = \exp(-2\,\Omega_{i,k}(s, b))$, is the probability that the initial projectiles (i, k) reach the final state interaction unchanged, regardless of the initial state re-scatterings.

The first approach is to use the eikonal approximation for Ω in which

$$\Omega_{i,k}^P(r_\perp, Y - Y_0, b) = \int d^2b' \, d^2b'' \, g_i\left(\boldsymbol{b}', m_i\right) G^{\text{dressed}}$$
$$\times \left(G_P\left(r_\perp, Y - Y_0, \boldsymbol{b}''\right)\right) g_k\left(\boldsymbol{b} - \boldsymbol{b}' - \boldsymbol{b}'', m_k\right) \tag{9}$$

where m_i denote the masses, which is introduced phenomenologically to determine the b dependence of g_i (see below). However, we do not have any reason to trust the eikonal approximation, which we discovered, is not sufficient to fit the experimental data.

Table 1
Fitted parameters of the model. The parameters for the Pomeron channel are taken from Ref. [2,5]. Reggeons parameters were derived from a fit to the data at low energies (see Fig. 2). The value of $\alpha_{P'}(0) = \alpha_\omega(0)$ is fixed from our fit for the DIS structure function F_2 [2]. α'_R is taken to be equal to 1 GeV^{-2} which comes from the reggeon trajectories in the resonance region. $\chi^2/d.o.f. = 1.2$.

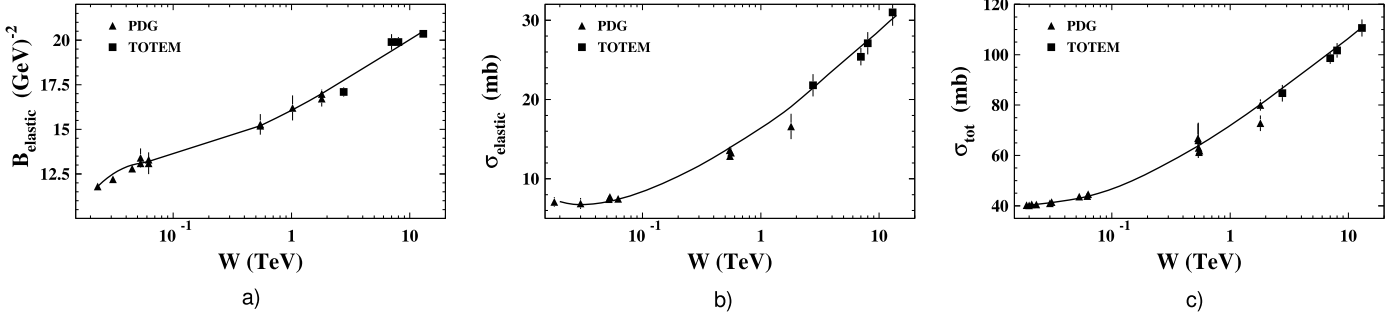|	λ	ϕ_0 (GeV^{-2})	g_1 (GeV^{-1})	g_2 (GeV^{-1})	m (GeV)	m_1 (GeV)	m_2 (GeV)	β
Pomeron	0.38	0.0019	110.2	11.2	5.25	0.92	1.9	0.58
	$\alpha_{P'}(0)$	$\alpha_\omega(0)$	$g_1^{P'}$ (GeV^{-1})	$g_2^{P'}$ (GeV^{-1})	$R_{0,1}^{P'}$ (GeV^{-1})	$R_{0,2}^{P'}$ (GeV^{-1})	$g_1^\omega = g_2^\omega$ (GeV^{-1})	$R_{0,1}^\omega = R_{0,2}^\omega$ (GeV^{-1})
Reggeons	0.55	0.55	2.937	5.365	2.18	8.633	3.61	2.611

Fig. 2. The energy behavior of $\sigma_{tot}, \sigma_{el}$ and the slope B_{el} for proton–proton scattering in our model. Data are taken from Refs. [12,35].

4. The model: phenomenological feedback for the theoretical approach

We propose a more general approach, which takes into account the new small parameters, that are determined by fitting to the experimental data (see Table 1 and Fig. 1 for notation):

$$G_{3P}\Big/g_i(b=0) \ll 1; \qquad m \gg m_1 \text{ and } m_2. \qquad (10)$$

The first equation means that we can develop the approach for the Pomeron interactions in which only terms that are proportional to $g_i G_P G_{3P}$ are taken into account, while the contributions of the order of $G_{3P} G_P G_{3P}$ are negligibly small. Therefore, using the first small parameter of Eq. (10), we see that the main contribution stems from the net diagrams shown in Fig. 1(b) [31].

The second equation in Eq. (10) leads to the fact that b'' in Eq. (9) is much smaller than b and b', therefore, Eq. (9) can be re-written in a simpler form

$$\Omega_{i,k}^P(r_\perp, Y - Y_0, b) = \underbrace{\left(\int d^2 b'' \, G^{\text{dressed}}\left(G_P\left(r_\perp, Y - Y_0, \boldsymbol{b}''\right)\right)\right)}_{\tilde{G}^{\text{dressed}}(r_\perp, Y-Y_0)}$$
$$\times \int d^2 b' g_i\left(\boldsymbol{b}'\right) g_k\left(\boldsymbol{b} - \boldsymbol{b}'\right). \qquad (11)$$

We can see that the proton–proton interaction is similar to the nucleus–nucleus interaction. For a nucleus interaction $g_i \propto A^{1/3} \gg G_{3P}$ and $R_A \gg R_N$, where R_A and R_N denote the nucleus and nucleon radii, respectively. Eq. (10) shows the same hierarchy of the vertices and radii is present in proton proton scattering. The sum of these diagrams [5] leads to the following expression for $\Omega_{i,k}^P(s, b)$

$$\Omega_{i,k}^P(r, Y - Y_0; b)$$
$$= \int d^2 b' \frac{g_i\left(\boldsymbol{b}'\right) g_k\left(\boldsymbol{b} - \boldsymbol{b}'\right) \tilde{G}^{\text{dressed}}(r, Y - Y_0)}{1 + G_{3P}\, \tilde{G}^{\text{dressed}}(r, Y - Y_0)\left[g_i\left(\boldsymbol{b}'\right) + g_k\left(\boldsymbol{b} - \boldsymbol{b}'\right)\right]};$$
$$g_i(b) = g_i\, S_p\left(b; m_i\right); \qquad (12)$$

where

$$S_p(b, m_i) = \frac{1}{4\pi} m_i^3\, b\, K_1(m_i b) \xrightarrow{\text{Fourier image}} \frac{1}{\left(1 + Q_T^2/m_i^2\right)^2};$$
$$\tilde{G}^{\text{dressed}}(r, Y - Y_0) = \int d^2 b\, G^{\text{dressed}}(r, Y - Y_0, b). \qquad (13)$$

Formula of Eq. (12) describes the net diagrams where the Green function of the BFKL Pomeron is replaced by the dressed Pomeron Green function, as is shown in Fig. 1(b).

The impact parameter dependence of $S_p(b, m_i)$ is purely phenomenological, Eq. (13) which has a form of the electromagnetic proton form factor, leads to the correct $(\exp(-\mu b))$ behavior at large b [29], and has the correct behavior at large Q_T, which has been calculated in the framework of perturbative QCD [32]. We wish to draw the reader's attention to the fact that m_1 and m_2 are the two dimensional scales in a hadron, which in the framework of the constituent quark model, we assign to the size of the hadron ($R_h \propto 1/m_1$), and the size of the constituent quark ($R_Q \propto 1/m_2$). Note that $\tilde{G}^{\text{dressed}}(Y - Y_0)$ does not depend on b. In all previous formulae, the value of the triple BFKL Pomeron vertex is known: $G_{3P} = 1.29$ GeV^{-1}.

5. Theoretical background: the secondary Reggeons

Unfortunately, perturbative QCD cannot lead to an understanding of the nature of the secondary Regge poles, which describe the energy behavior of quasi-elastic processes with non vacuum quantum numbers in t-channel. We have abundant experimental confirmations of these contributions, as well as acumen, that the existence of secondary Reggeons is ultimately related to the production of a rich variety of resonances. Therefore, the secondary Reggeons remain an open question, that has to be solved in non-perturbative QCD. At the moment we assume the pure phenomenological approach for the contribution of the secondary Reggeons, replacing Ω^P by the sum: $\Omega^P + \Omega^P$, where Ω^P is equal to

$$\Omega_{i,k}^R = \Omega_{i,k}^{P'} \pm \Omega_{i,k}^\omega \quad \text{with}$$
$$\Omega_{i,k}^{P'(\omega)} = \frac{g_i^{P'(\omega)} g_k^{P'(\omega)}}{\pi R_{i,k}^2(Y)} e^{-\frac{b^2}{R_{i,k}^2(Y)}} \left(\frac{s}{s_0}\right)^{\alpha_{P'(\omega)}(0)}. \qquad (14)$$

Sign $+$ $(-)$ in Eq. (14) relates to proton–antiproton (proton–proton) scattering.

$$R_{i,k}^2(Y) = R_{0,i}^2 + R_{0,k}^2 + \alpha_R' Y. \qquad (15)$$

We chose the intercepts of $\alpha_{P'}(0)$ and $\alpha_\omega(0)$ to be equal, in the spirit of the duality between resonances and Regge exchanges that leads to signature degeneracy.

All parameters were determined from a fit of the relevant experimental data. In our attempts to describe DIS data [1] we fixed $\alpha_{P'}(0) = 0.55$. It should be stressed that Eq. (14) is written for the imaginary part of the amplitude.

We determine the real part of the amplitude, using dispersion relations.

6. Physical observables

In this paper we concentrate our efforts on the description of the total, elastic cross sections and the elastic slope in the region of low energies starting from $W = 30$ GeV.

For the completeness of presentation, we give the expressions for the physical observables that we used in this paper. They can be written as follows

elastic amplitude :

$$a_{el}(s, b) = i(\alpha^4 A_{1,1} + 2\alpha^2 \beta^2 A_{1,2} + \beta^4 A_{2,2}); \qquad (16)$$

elastic cross section :

$$\sigma_{tot}(s) = 2 \int d^2 b \, a_{el}(s, b); \quad \sigma_{el}(s) = \int d^2 b \, |a_{el}(s, b)|^2;$$

elastic slope :

$$B_{el}(s) = \frac{1}{2} \int d^2 b \, b^2 a_{el}(s, b) \Big/ \int d^2 b \, a_{el}(s, b).$$

As has been mentioned, we wish to study the energy behavior of the parameter $\rho = \mathrm{Re}/\mathrm{Im}$. To find the real part of the amplitude we use the dispersion relation as suggested in Ref. [33] (see also Ref. [34]). For proton–proton scattering the expression for ρ has the form:

$$\rho = \frac{1}{\sigma_{tot}^{pp}} \frac{\pi}{4} \left\{ \frac{d}{d \ln(s/s_0)} \left(\sigma_{tot}^{pp} + \sigma_{tot}^{\bar p p} \right) + \frac{1}{s} \frac{d}{d \ln(s/s_0)} \right.$$
$$\left. \times \left(s \left(\sigma_{tot}^{pp} - \sigma_{tot}^{\bar p p} \right) \right) \right\}. \qquad (17)$$

In Eq. (17) we replace $\tan\left(\frac{1}{2}\pi \frac{d}{d \ln s}\right)$ by $\frac{1}{2}\pi \frac{d}{d \ln s}$ since both $\frac{d}{d \ln(s/s_0)}\left(\sigma_{tot}^{pp} + \sigma_{tot}^{\bar p p}\right)$ and $\frac{1}{s}\frac{d}{d \ln(s/s_0)}\left(s\left(\sigma_{tot}^{pp} - \sigma_{tot}^{\bar p p}\right)\right)$ turn out to be small.

From Eq. (8), Eq. (16) and Eq. (17) one can see that $\rho \propto \int d^2 b \frac{d\Omega_{i,k}(s,b)}{d \ln s} \exp\left(-\Omega_{i,k}(s, b)\right) \xrightarrow{s \gg s_0} 0$. This equation shows that ρ is small and decreases at high energies. The values of ρ crucially depend on the amount of the shadowing which we incorporated in the model. As we see below, our model, based on the CGC approach, provides the degree of shadowing which is in accord with the experimental data. On the other hand, the small value and the behavior of ρ provides hope that we can find the odderon contribution in ρ at high energies.

7. Results of the fit

The parameters, related to the Pomeron interaction (see first row in Table 1), have been determined in our previous papers (see Refs. [1,2]) by fitting to very high energies $W = 0.574 \div 13$ TeV data. In this paper we extract the parameters of the
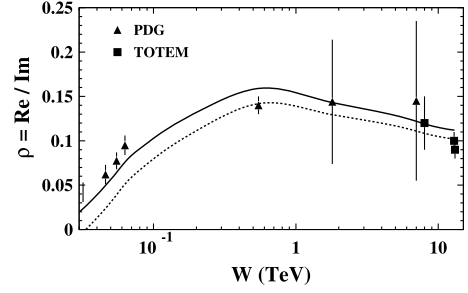

Fig. 3. $\rho = \mathrm{Re}/\mathrm{Im}$ for proton–proton scattering versus $W = \sqrt{s}$. Data are taken from PDG [35] and from the TOTEM papers [12]. The solid line shows our predictions while the dotted one presents the estimates for the value of ρ, when adding the odderon contribution 1.1 mb at $W = 13$ TeV, to our model.

secondary reggeons using data for σ_{tot}, σ_{el} B_{el} at low energies $W = 20 \div 574$ GeV. In doing so we pursued two goals: to provide independent estimates of the value of the secondary reggeon contribution for $W \geq 0.574$ TeV; and to organize the fit in a such way that the abundance of more precise data at lower energies will not spoil the fit at high energies.

In addition, we fix the intercept of the P'-Reggeon to the same value we found in the DIS [2] fit. The parameters of the secondary reggeons that we extracted from the fit, are shown in the second row of Table 1. Using these parameters we estimate that the secondary reggeon contribution for $W \geq 0.574$ TeV is negligibly small ($<1\%$). It means that the behavior of ρ at these energies is determined only by the Pomeron contributions, assuming that there is no odderon contribution.

In Fig. 3 we present our prediction for ρ. One can see that even without an additional odderon contribution our model predicts that at $W = 13 \, TeV$ $\rho \approx 0.1$. This result is in a good agreement with the TOTEM data.

8. Conclusions

Fig. 3 shows the main result of this paper: our model leads to the $\rho = \mathrm{Re}/\mathrm{Im} \approx 0.1$ at $W = 13$ TeV. It reproduces the TOTEM data without assuming the additional contribution of the odderon. On the other hand the TOTEM data, in the framework of our model, allows an odderon contribution of the order of 1 mb at $W = 13$ TeV. Since the odderon gives the real contribution, it does not affect our fitting procedure. We expect that the odderon contribution does not depend on energy and will lead to smaller values of ρ at low energies as is shown by the dotted line in Fig. 3. Such a contribution does not describe the data at low energies, in spite of improving the agreement with the data at high energies, including the TOTEM measurements.

In perturbative QCD the odderon contribution can only depend logarithmically on energy. However, it is shown in Ref. [3,22], using the solution of Ref. [36], that the shadowing, non-linear corrections suppress the energy behavior of the odderon at high energies, generating the survival probability damping factor. In our model the odderon contribution to ρ is screened as

$$\rho_{\text{odderon}} = \int d^2 b \, O(s, b) \left(1 - a_{el}(s, b) \right) \Big/ \int d^2 a_{el}(s, b). \qquad (18)$$

Eq. (18) shows that the odderon contribution is suppressed at high energies qualitatively in the same way as the Pomeron contribution to ρ. Therefore, we are of the opinion that ρ is not the appropriate observable to determine the existence of the odderon. In the model we can estimate the contribution of the odderon at lower energies taking into account that the impact parameter dependence of the odderon which is expected to be concentrated at

smaller b than that for the Pomeron [37]. In this case Eq. (18) takes the form

$$\rho_{\text{odderon}} = \int d^2b\, O(s,b)\left(1 - a_{el}(s,b=0)\right)\bigg/\int d^2 a_{el}(s,b). \tag{19}$$

Numerically, Eq. (19) leads to $\int d^2b\, O(s,b) = 23$ mb at $W = 13$ TeV. Since $O(s,b)$ does not depend on energy, this large value means that the odderon term should be essential at lower energies, and should be taken in consideration together with the secondary reggeons. Indeed, at $W = 21.2$ GeV the odderon contribution from Eq. (19) gives Re $A(S, t=0) = 8.8$ mb while the contribution of the secondary reggeons to the total cross is equal to 14.6 mb. Therefore, we do not think that ρ at high energies is an appropriate observable for determining the odderon contribution.

In this paper we demonstrated that two effects: the decrease with energy as well as the value of ρ; and the suppression of the odderon contribution stem from the amount of the shadowing correction that is originates from the CGC/saturation approach of our model.

As we have discussed our model also describes the wide range of the experimental observables. We believe that these successes provide a strong argument in favour of the CGC/saturation approach.

Acknowledgements

References

[1] E. Gotsman, E. Levin, I. Potashnikova, Phys. Lett. B 781 (2018) 155, arXiv:1712.06992 [hep-ph].
[2] E. Gotsman, E. Levin, I. Potashnikova, Eur. Phys. J. C 77 (9) (2017) 632, arXiv:1706.07617 [hep-ph].
[3] Yuri V. Kovchegov, Eugene Levin, Quantum Choromodynamics at High Energies, Cambridge Monographs on Particle Physics, Nuclear Physics and Cosmology, Cambridge University Press, 2012.
[4] E. Gotsman, E. Levin, U. Maor, Eur. Phys. J. C 75 (1) (2015) 18, arXiv:1408.3811 [hep-ph].
[5] E. Gotsman, E. Levin, U. Maor, Eur. Phys. J. C 75 (5) (2015) 179, arXiv:1502.05202 [hep-ph].
[6] E. Gotsman, E. Levin, U. Maor, Phys. Lett. B 746 (2015) 154, arXiv:1503.04294 [hep-ph].
[7] E. Gotsman, E. Levin, U. Maor, Eur. Phys. J. C 75 (11) (2015) 518, arXiv:1508.04236 [hep-ph].
[8] E. Gotsman, E. Levin, U. Maor, arXiv:1510.07249 [hep-ph].
[9] E. Gotsman, E. Levin, U. Maor, S. Tapia, Phys. Rev. D 93 (7) (2016) 074029, arXiv:1603.02143 [hep-ph].
[10] E. Gotsman, E. Levin, Phys. Rev. D 95 (1) (2017) 014034, arXiv:1611.01653 [hep-ph].
[11] E. Gotsman, E. Levin, Phys. Rev. D 96 (7) (2017) 074011, arXiv:1705.07406 [hep-ph].
[12] G. Antchev, et al., TOTEM Collaboration, First measurement of elastic, inelastic and total cross-section at $\sqrt{s} = 13$ TeV by TOTEM and overview of cross-section data at LHC energies, CERN-EP-2017-321, CERN-EP-2017-321-V2, arXiv:1712.06153 [hep-ex];
G. Antchev et al., First determination of the ρ parameter at $\sqrt{s} = 13$ TeV ρ probing the existence of a colourless three-gluon bound state, CERN-EP-2017-335, Submitted to: Phys. Rev.
[13] V.A. Khoze, A.D. Martin, M.G. Ryskin, Elastic and diffractive scattering at the LHC, arXiv:1806.05970 [hep-ph].
[14] W. Broniowski, L. Jenkovszky, E. Ruiz Arriola, I. Szanyi, Hollowness in pp and $p\bar{p}$ scattering in a Regge model, arXiv:1806.04756 [hep-ph].
[15] S.M. Troshin, N.E. Tyurin, Implications of the $\rho(s)$ measurements by TOTEM at the LHC, arXiv:1805.05161 [hep-ph].
[16] E. Martynov, B. Nicolescu, Evidence for maximality of strong interactions from LHC forward data, arXiv:1804.10139 [hep-ph].
[17] M. Broilo, E.G.S. Luna, M.J. Menon, Phys. Lett. B 781 (2018) 616, arXiv:1803.07167 [hep-ph].
[18] Y.M. Shabelski, A.G. Shuvaev, Eur. Phys. J. C 78 (6) (2018) 497, arXiv:1802.02812 [hep-ph].
[19] V.A. Khoze, A.D. Martin, M.G. Ryskin, Phys. Lett. B 780 (2018) 352, arXiv:1801.07065 [hep-ph].
[20] V.A. Khoze, A.D. Martin, M.G. Ryskin, Phys. Rev. D 97 (3) (2018) 034019, arXiv:1712.00325 [hep-ph].
[21] J. Bartels, L.N. Lipatov, G.P. Vacca, Phys. Lett. B 477 (2000) 178, arXiv:hep-ph/9912423.
[22] Y.V. Kovchegov, L. Szymanowski, S. Wallon, Phys. Lett. B 586 (2004) 267, arXiv:hep-ph/0309281.
[23] T. Altinoluk, A. Kovner, E. Levin, M. Lublinsky, J. High Energy Phys. 1404 (2014) 075, https://doi.org/10.1007/JHEP04(2014)075, arXiv:1401.7431 [hep-ph].
[24] A.H. Mueller, B. Patel, Nucl. Phys. B 425 (1994) 471;
A.H. Mueller, G.P. Salam, Nucl. Phys. B 475 (1996) 293, arXiv:hep-ph/9605302;
G.P. Salam, Nucl. Phys. B 461 (1996) 512;
E. Iancu, A.H. Mueller, Nucl. Phys. A 730 (2004) 460, arXiv:hep-ph/0308315;
494, arXiv:hep-ph/0309276.
[25] I. Balitsky, arXiv:hep-ph/9509348;
I. Balitsky, Phys. Rev. D 60 (1999) 014020, arXiv:hep-ph/9812311;
Y.V. Kovchegov, Phys. Rev. D 60 (1999) 034008, arXiv:hep-ph/9901281.
[26] E. Levin, J. High Energy Phys. 1311 (2013) 039, https://doi.org/10.1007/JHEP11(2013)039, arXiv:1308.5052 [hep-ph].
[27] I. Gradstein, I. Ryzhik, Table of Integrals, Series, and Products, fifth edition, Academic Press, London, 1994.
[28] A. Kovner, U.A. Wiedemann, Phys. Rev. D 66 (2002) 051502,034031, arXiv:hep-ph/0112140, arXiv:hep-ph/0204277;
A. Kovner, U.A. Wiedemann, Phys. Lett. B 551 (2003) 311, arXiv:hep-ph/0207335.
[29] M. Froissart, Phys. Rev. 123 (1961) 1053;
A. Martin, Scattering Theory: Unitarity, Analitysity and Crossing, Lecture Notes in Physics, Springer-Verlag, Berlin-Heidelberg-New-York, 1969.
[30] M.L. Good, W.D. Walker, Phys. Rev. 120 (1960) 1857.
[31] E. Gotsman, E. Levin, U. Maor, Eur. Phys. J. C 71 (2011) 1553, arXiv:1010.5323 [hep-ph].
[32] G.P. Lepage, S.J. Brodsky, Phys. Rev. Lett. 43 (1979) 545;
Phys. Rev. Lett. 43 (1979) 1625.
[33] J.B. Bronzan, G.L. Kane, U.P. Sukhatme, Phys. Lett. B 49 (1974) 272.
[34] C.A.S. Bahia, M. Broilo, E.G.S. Luna, Int. J. Mod. Phys. Conf. Ser. 45 (2017) 1760064;
P.D.B. Collins, An Introduction to Regge Theory and High-Energy Physics, Cambridge Monographs on Mathematical Physics, Cambridge Univ. Press, Cambridge, UK, 2009;
S. Donnachie, H.G. Dosch, O. Nachtmann, P. Landshoff, Pomeron physics and QCD, Camb. Monogr. Part. Phys. Nucl. Phys. Cosmol. 19 (2002) 1.
[35] M. Tanabashi, et al., Particle Data Group, The Review of Particle Physics, Phys. Rev. D 98 (2018) 030001, 2018.
[36] E. Levin, K. Tuchin, Nucl. Phys. B 573 (2000) 833, arXiv:hep-ph/9908317.
[37] J. Kwiecinski, M. Praszalowicz, Phys. Lett. B 94 (1980) 413.